Military Technical College
Kobry El-Kobbah,
Cairo, Egypt

6th International Conference
on Electrical Engineering
ICEENG 2008

Antenna gain optimization for LEO satellites using a genetic algorithm

By

H. H. El-Banna* A.A. Mitkees** A. M. Allam ** M.M. Mokhtar**

Abstract:

A rectangular planar array antenna synthesis technique based on Genetic Algorithm optimization is used to achieve sufficient link margin for low earth orbit (LEO) satellites antenna, by adjusting the antenna gain.
A genetic algorithm (GA) is used to optimize the array excitation. Thinning [1] of elements is used with different excitation techniques.
A phased array antenna with rectangular aperture and $\cos^{1.5}\theta$ elements power pattern is assumed.

Keywords:

Phased Array Antennas, LEO Satellite Antennas, Genetic Algorithm

---

* Ph. D. Student, Egyptian Armed Forces
** Prof. Dr., Egyptian Armed Forces

1. Introduction:

Slant range path-loss variation at geostationary orbit (GEO) is only 1.3 dB from nadir to 0^o elevation edge of coverage (EOC) and usually can be ignored [2], but the slant range path-loss variation for LEO satellites is very high. At an altitude 850 Km, for example, the slant range path loss variation varies around 9 dB from nadir to EOC [3].
In order to achieve isoflux illumination and constant link margin, antenna gain must increase as a function of the angle away from nadir on the earth surface.
Genetic algorithm [4, 5], has a high ability in global optimization. It is an increasingly popular optimization method being applied to many fields, including electromagnetic optimization problems.
Using genetic algorithm to synthesize array pattern has no limitation on lattice shapes and aperture shapes. It can synthesize planar array with arbitrary geometry and generating arbitrary patterns. Compared with other numerical methods [6, 7], this approach has unique features to treat complicated problems as arrays.
Thinning (turning some elements on and the other off) of the elements is one of the simplest excitation techniques to get the objective directivity of the antenna [8].
Genetic algorithm is used to get all of the optimum distribution of the on and off elements, nonuniform excitations of the elements, also the achieved directivity in case of uniform excitations. Steering of the beam is achieved by the appropriate phase shifters.

2. Problem formulation:

An S-band 8 x 8 planar array antenna is designed to be placed on a face of a three axis stabilized cubic sun-synchronous satellite; the face which faced to the earth. The objective from this work is to adjust the antenna gain to compensate the slant range variations from nadir till the EOC to achieve a constant link margin.
The far-field radiation pattern $F(\theta,\phi)$ at an angle from the array broadside is given by [9]:

$$F(\theta,\phi)=EF(\theta).AF(\theta,\phi) \qquad (1)$$

where

$$EF(\theta)=\cos^{1.5}(\theta) \qquad (2)$$

is the assumed element radiation pattern, and

$$AF(\theta,\phi) = \sum_{n=1}^{N}\sum_{m=1}^{M} a_{mn} e^{jk[md_x(u-u_0)+nd_y(v-v_0)]} \tag{3}$$

is the array radiation pattern, described by the following parameters;

$M, N =$ number of elements in the x and y-direction, respectively,
$a_{mn} =$ amplitude excitation coefficient of the *mn* element,
$d_x =$ separation distance between two successive elements in the x-direction,
$d_y =$ separation distance between two successive elements in the y-direction,
$kd_x u_0 =$ element-to-element phase shift in the x- direction,
$kd_y v_0 =$ element-to-element phase shift in the y- direction,
$u = \sin\theta\cos\phi$, $v = \sin\theta\sin\phi$, $u_0 = \sin\theta_0\cos\phi_0$, $v_0 = \sin\theta_0\sin\phi_0$,
$\theta_0 =$ the desired direction of maximum, measured from antenna broadside,
$\phi_0 =$ the desired direction of maximum, measured from the x- axis in the x-y plane.

As the satellite go away w.r.t. the ground station the slant range is increased, so, the antenna directivity should be increased to keep fixed link margin, as follows:

$$DD_r(\theta_0,\phi_0) = D_0\left[\frac{R_s(\theta_0,\phi_0)}{h}\right]^2 \tag{4}$$

where

DD_r : the desired directivity (ratio) at each slant range,
D_0 : the required directivity (ratio) at nadir, is taken equal 5.
h : the satellite altitude,
R_s : the slant range from the earth station to the satellite, calculated as follows:

$$R_s = \sqrt{-2R_e(R_e+h)\cos(\gamma) + (R_e+h)^2 + R_e^2}$$

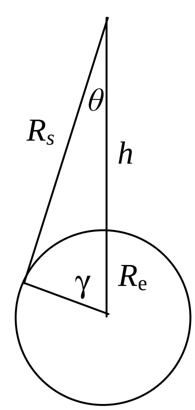

R_e : earth radius
γ : earth central angle, calculated as follows:

$$\gamma = \sin^{-1}\left(\frac{(R_e+h)\sin(\theta)}{R_e}\right) - \theta$$

Also, the general formula of the directivity can be calculated from the antenna field pattern [9], as follows:

$$D(\theta_0,\phi_0)=\frac{\left|F(\theta_0,\phi_0)\right|^2}{\frac{1}{4\pi}\int_{\text{all space}}\left|F(\theta,\phi)\right|^2 d\Omega} \qquad (5)$$

where $d\Omega=\sin\theta\, d\theta\, d\phi$.

The goal now is to achieve the optimum Directivity to be close as possible to the desired directivity. Genetic algorithm is used to get the optimum excitations to get the optimum directivity.

3. Genetic algorithm optimization:

Genetic algorithm [10] optimizers are robust stochastic search methods modeled on the principles and concepts of natural selection and evolution. As an optimizer, the powerful heuristic of the GA is effective at solving complex combinatorial and related problems. GA optimizers are particularly effective when the goal is to find an approximate global maximum in a high-dimension, multi–modal function domain.

A genetic algorithm using population decimation, crossover, and mutation was used to generate new individuals as shown in *Figure (1)*.
The fitness function is used to determine which of the selected parents better fit to produce offspring for the next generation, to determine which individuals are replaced each generation, and finally get the best chromosome which satisfy the objective.
The fitness or the objective function in this problem is:

$$f=\left|D(\theta_0,\phi_0)-DD_r(\theta_0,\phi_0)\right| \qquad (6)$$

The optimum of f equals zero, so the objective is the minimization of f.
Genes are the excitation coefficients of each element. Excitation is amplitude and phase, the phase is pre-calculated to steer the beam to the desired direction, and the amplitude of each element is achieved by GA.
It is known that, the maximum directivity is achieved when uniform excitations are used.
Thinning and nonuniform excitations are two approaches, used to achieve the optimum directivity. Genes are zeros and ones in case of thinning. And each gene is represented by 32 bit in case of nonuniform excitations.

Thinning an array means turning off some elements in a uniformly spaced or periodic array to create a desired amplitude density across the aperture. An element connected to the feed network is “on”, and an element connected to a matched or dummy load is “off”. Thinning an array to produce the desired directivity is much simpler than the more general problem of nonuniform excitations of the elements.
Each chromosome is represented by a 2-D array, and the population is a 3-D array. Crossover as shown in *Figure (2)*, and the probability of mutation is taken 0.05 of the whole population size. Initial population generation technique, crossover technique, and mutation have a big effect of the convergence to the optimum solution.

4. Simulation results:

Consider a case of a sun synchronous LEO satellite of altitude 850 Km, in a ground track with ϕ_0 equals zero. θ_0 changes from nadir (θ_0 = zero) till the EOC [11] equals 60^o. *Figures (4)* through *(9)* show the normalized far field pattern in case of thinned elements at different θ_0 which simulate the movement of the satellite.
The results as expected, as the satellite go away from nadir till the EOC the numbers of ON elements increased, and the pattern beamwidth decreases. *Tables (1)* through *(6)* show the ON and OFF elements in the array. In the tables, the first top left element represents the element at the origin, the elements in the same row in the y-direction, and the elements in the same column in the x-direction of the planar array.
Figures (10) through *(14)* show the normalized far field pattern in case of non-uniform excited elements at different θ_0. *Tables (7)* through *(11)* show the excitation coefficients of the elements at different θ_0. The dynamic range, DR, of the excitation coefficients are under constrains to be easy to realize. *Figure (3)* shows the desired and achieved directivity in case of uniform, thinning, and non-uniform excitations. Thinning of elements gives optimum results to achieve the desired directivity by using GA.

5. Conclusions:

An antenna array of 8 x 8 elements is used to be fitted on the surface of a LEO satellite. By an easy way of excitations, thinning of the elements gives optimum results to achieve the desired directivity to achieve constant link margin during a certain ground track from the nadir till EOC.
GA is a powerful algorithm to achieve a certain objective, it is effective at solving complex combinatorial and related problems.

References:

[1] Randy L. Haupt, " *Thinned Arrays Using Genetic Algorithms,*" IEEE Trans. Antennas propagation, vol. AP.42, No. 7, pp. 993-999,1994.
[2] Gary D. Gordon and Walter L. Morgan, *principles of Communications Satellites,* John Willy & Sons, Inc. 1993.
[3] Sherman, K. N., "*phased array shaped multi-beam optimization for LEO satellite communications using a genetic algorithm,*" International Conference on Phased Array Systems and Technology, Dana Point CA, USA, 21-25, pp. 501-504, May 2000
[4] J. Michael Johnson and Yahya Rahmat-Samii, "*Genetic Algorithms in Engineering Electromagnetics,*" IEEE Trans. Antennas propagation, vol. 39, No. 4, pp. 7 -21, August 1997.
[5] Randy L. Haupt, "*An Introduction to Genetic Algorithms for Electromagnetics,*" IEEE Trans. Antennas propagation, vol. 37, No. 2, pp. 7 -15, April (1995).
[6] Olen, C. A. and RT. Compton, Jr, "*A numerical pattern synthesis algorithm for arrays,*" IEEE Trans. Antennas propagation, vol. 38, No. 10, pp. 1666-1676, 1990.
[7] Zhou, P. Y. P. and M. A. Ingram, "*pattern synthesis for arbitrary arrays using an adaptive method,*" IEEE Trans. Antennas propagation, vol. 47, No. 5, pp. 862-869, 1999.
[8] Robert J. Mailloux, *Phased Array Antenna Handbook (2nd ed.),* Artech House, 2005.
[9] Richard C. Jonson, *Antenna Engineering Handbook (3rd ed.)*, McGraw-Hill, 1993.
[10] Hazem H. El-Banna," *Sidelobe Cancellation in antenna arrays for Radar applications,*" M.sc. thesis, ch.4, 2001
[11] E. Jacobs, J. M. Stacey, "*Earth Footprints of Satellite Antennas,*" IEEE Trans. on Aerospace and Electronic Systems, vol. AES. 7, No. 2, pp. 235-242, March (1971).

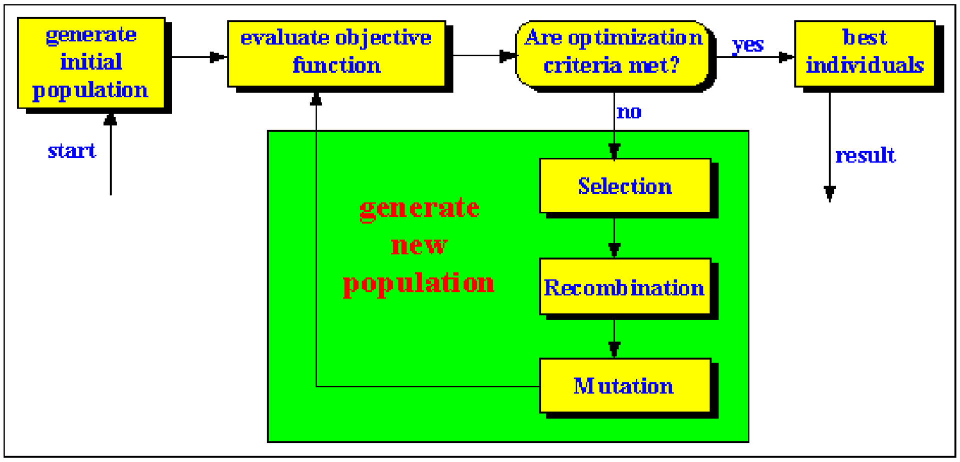

Figure (1): *A block diagram of a simple genetic-algorithm optimizer*

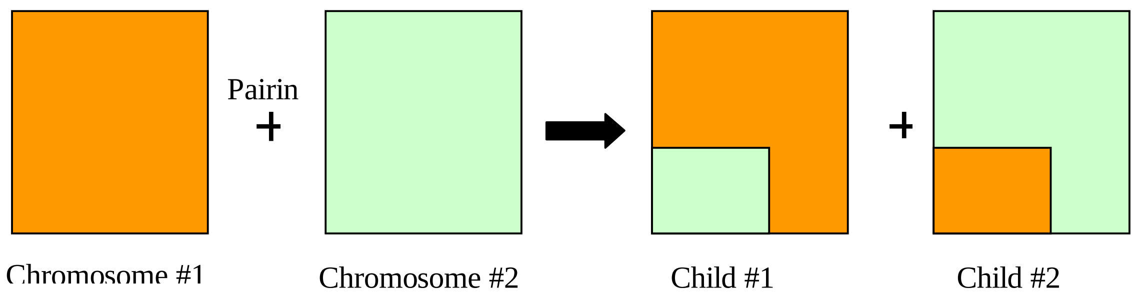

Figure (2): *The used technique of the crossover area in the case of planar array*

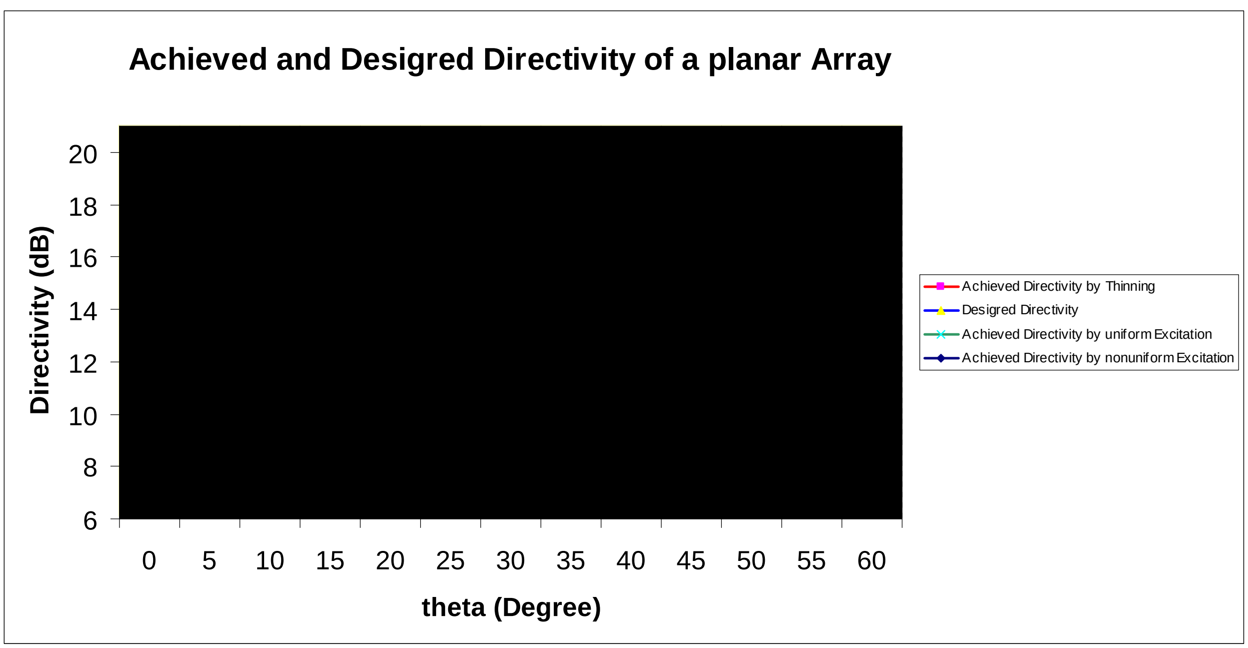

Figure (3): *The Achieved and desired Directivity of the planar array*

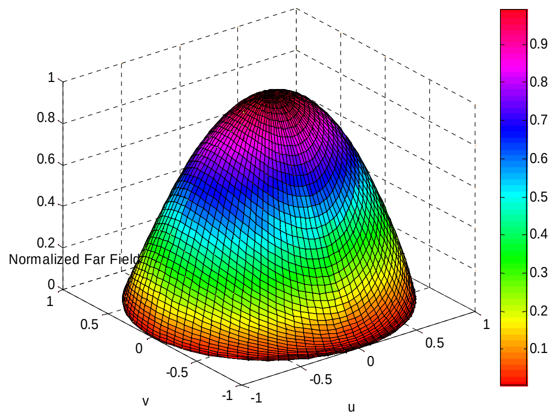

Figure (4): *The Normalized far field pattern at theta 0 deg.*

Table (1): *The thinned elements at theta 0 deg.*

1	1	0	0	0	0	0	0
0	0	0	0	0	0	0	0
0	0	0	0	0	0	0	0
0	0	0	0	0	0	0	0
0	0	0	0	0	0	0	0
0	0	0	0	0	0	0	0
0	0	0	0	0	0	0	0
0	0	0	0	0	0	0	0

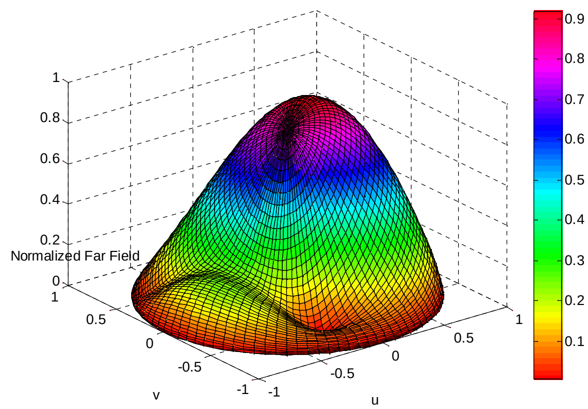

Figure (5): *The Normalized far field pattern at theta 25 deg.*

Table (2): *The thinned elements at theta 25 deg.*

1	0	0	0	0	0	0	0
1	1	0	0	0	0	0	0
0	0	0	0	0	0	0	0
0	0	0	0	0	0	0	0
0	0	0	0	0	0	0	0
0	0	0	0	0	0	0	0
0	0	0	0	0	0	0	0
0	0	0	0	0	0	0	0

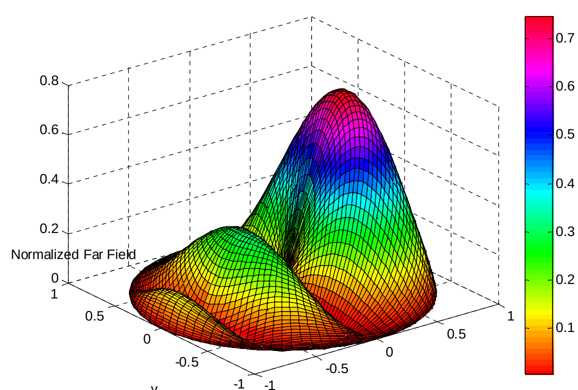

Figure (6): *The Normalized far field pattern at theta 40 deg.*

Table (3): *The thinned elements at theta 40 deg.*

1	1	0	0	0	0	0	0
1	1	0	0	0	0	0	0
1	1	0	0	0	0	0	0
0	0	0	0	0	0	0	0
0	0	0	0	0	0	0	0
0	0	0	0	0	0	0	0
0	0	0	0	0	0	0	0
0	0	0	0	0	0	0	0

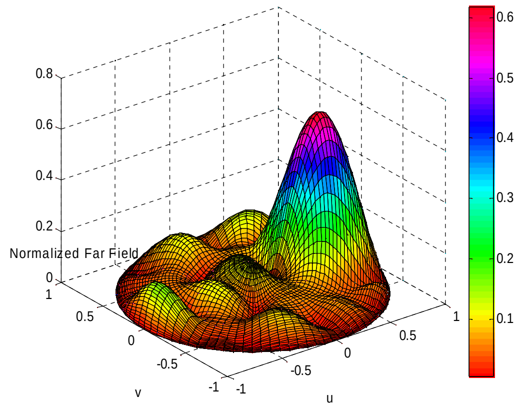

***Figure (7):** The Normalized far field pattern at theta 50 deg.*

***Table (4):** The thinned elements at theta 50 deg.*

1	0	1	0	0	0	0	0
1	1	1	1	0	0	0	0
1	1	1	1	0	0	0	0
1	1	0	1	0	0	0	0
0	0	0	0	0	0	0	0
0	0	0	0	0	0	0	0
0	0	0	0	0	0	0	0
0	0	0	0	0	0	0	0

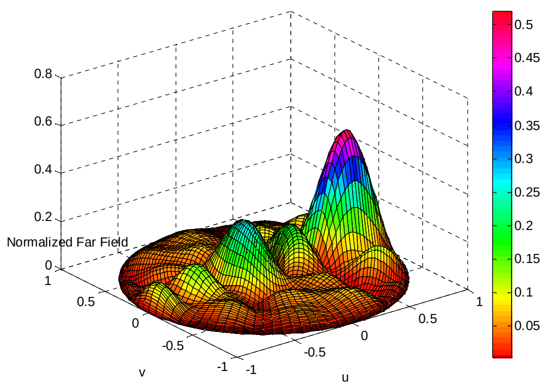

***Figure (8):** The Normalized far field pattern at theta 55 deg.*

***Table (5):** The thinned elements at theta 55 deg.*

1	1	0	1	1	1	0	0
1	0	1	0	1	1	0	0
1	1	1	1	1	1	0	0
1	0	1	1	1	1	0	0
1	0	1	1	1	1	0	0
0	0	0	0	0	0	0	0
0	0	0	0	0	0	0	0
0	0	0	0	0	0	0	0

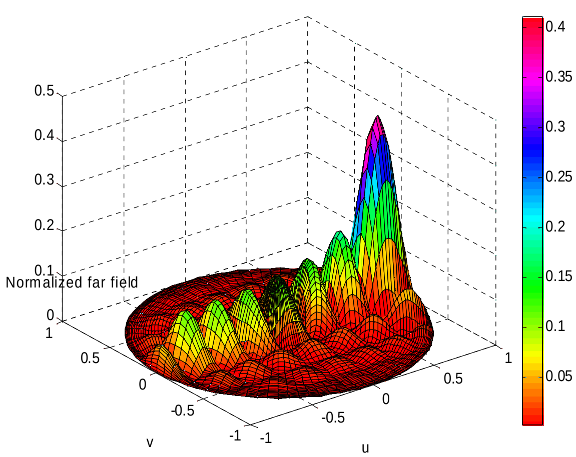

***Figure (9):** The Normalized far field pattern at theta 60 deg.*

***Table (6):** The thinned elements at theta 60 deg.*

1	1	1	1	1	1	1	1
1	1	1	1	1	1	1	1
1	1	1	1	1	1	1	1
1	1	1	1	1	1	1	1
1	1	1	1	1	1	1	1
1	1	1	1	1	1	1	1
1	1	1	1	1	1	1	1
1	1	1	1	1	1	1	1

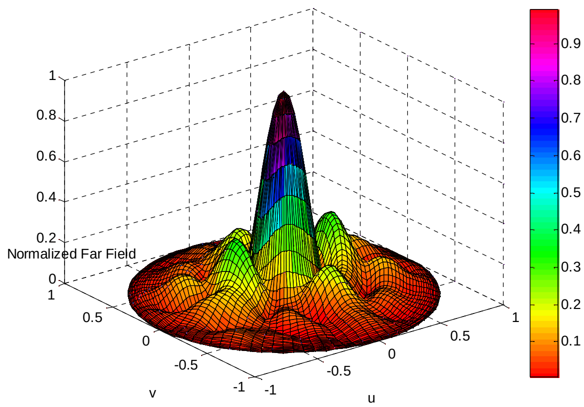

Figure (10): *The Normalized far field pattern at theta 0 deg., with non-uniform excitation.*

Table (7): *The excitation coefficients of each element, non-uniform excitation, theta 0* deg., DR= 60.5.

1.3207	48.162	65.856	13.202	9.6089	22.382	5.9097	9.4802
6.2507	9.6541	18.690	11.361	73.015	70.806	1.5488	2.7186
7.0569	1.3229	60.675	14.261	2.7367	28.649	63.173	8.7507
4.8189	33.563	42.719	10.433	12.827	15.862	4.5479	6.2575
28.507	9.0895	29.48	25.311	1.7024	1.2304	3.4368	25.230
4.6721	42.351	74.521	38.073	50.982	71.633	66.222	30.824
36.962	67.130	68.835	69.478	16.657	21.587	4.4259	14.277
3.0800	9.9702	54.711	4.7331	2.6893	8.9811	11.908	1.4336

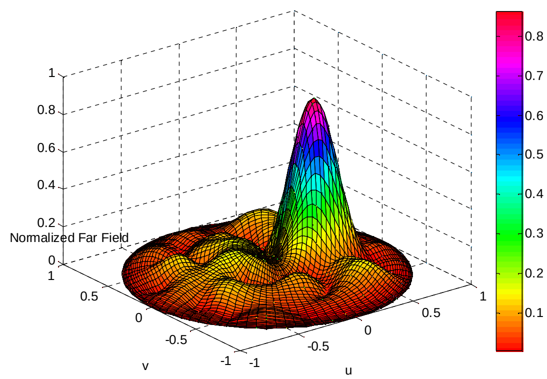

Figure (11): *The Normalized far field pattern at theta 25 deg., with non-uniform excitation.*

Table (8): *The excitation coefficients of each element, non-uniform excitation, theta 25 deg., DR= 71.6.*

19.099	2.6147	10.119	2.4815	12.100	18.455	6.7995	7.7006
5.9639	21.249	49.794	43.853	1.0903	11.047	6.2575	2.5470
1.9575	3.4345	7.1157	74.991	51.669	6.7882	64.853	20.551
31.764	1.8401	64.302	58.844	5.2344	19.383	19.078	6.3523
71.768	67.159	52.452	72.434	31.865	68.586	52.127	10.472
17.710	6.8108	65.714	70.402	8.6739	21.479	2.0931	6.6866
1.7114	1.0474	16.849	38.746	10.298	11.429	40.386	5.0380
7.7458	12.676	29.659	9.9612	3.6965	5.6952	12.658	12.527

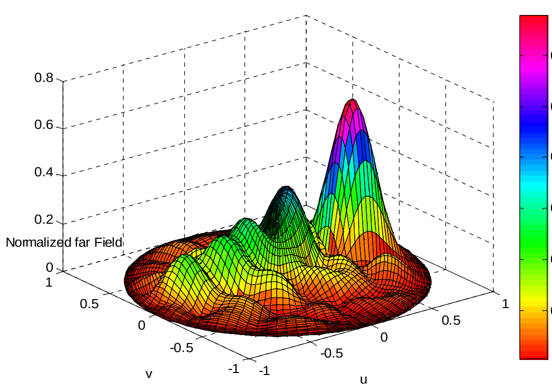

Figure (12): *The Normalized far field pattern at theta 40 deg., with non-uniform excitation.*

Table (9): *The excitation coefficients of each element, non-uniform excitation, theta 40 deg., DR= 74.6.*

4.3424	35.235	73.397	51.452	47.315	7.8293	4.9770	17.561
25.551	1.1920	24.801	32.920	12.540	22.866	2.7435	1.0045
1.9146	11.964	19.471	6.2733	3.8455	6.2846	44.496	11.136
1.5556	21.759	66.122	72.782	58.193	71.920	74.919	70.827
6.3952	14.516	3.2380	22.267	14.783	13.613	5.3248	2.3347
10.234	20.833	2.2466	13.423	13.667	68.119	8.5813	23.421
1.5781	7.5380	39.306	63.828	8.9043	29.668	6.1175	13.561
9.9477	26.095	40.463	31.743	8.6039	68.577	39.596	68.031

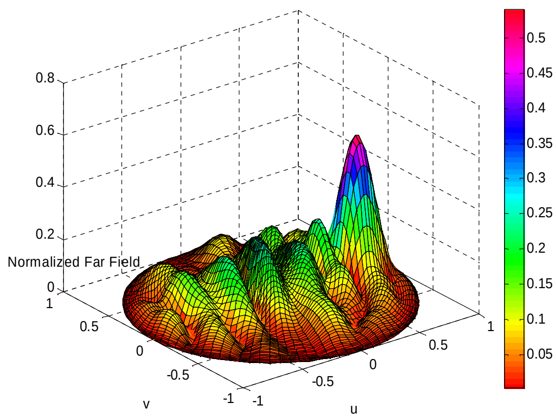

Table (10): *The excitation coefficients of each element, non-uniform excitation, theta 50 deg., DR= 76.4*

3.0284	1.4699	3.9203	2.4270	3.5116	6.6908	2.6761	1.3459
3.3101	1.8037	7.2965	2.2359	6.5078	2.1652	14.843	3.4964
2.9474	1.3151	5.9246	6.2862	7.4753	3.0340	1.8189	13.933
1.9043	1.8807	4.7216	6.2798	3.7494	3.9049	2.2786	2.7059
3.5049	8.5405	10.386	3.2372	21.03	3.6176	7.6585	8.3640
6.1012	8.2038	4.3419	10.245	10.319	0.9103	6.3873	7.6189
8.2507	1.5003	3.8401	8.9684	0.5183	12.530	2.3850	9.4244
1.4975	1.2907	5.6600	24.644	28.642	9.9318	5.3260	2.6160

Figure (13): *The Normalized far field pattern at theta 50 deg., with non-uniform excitation.*

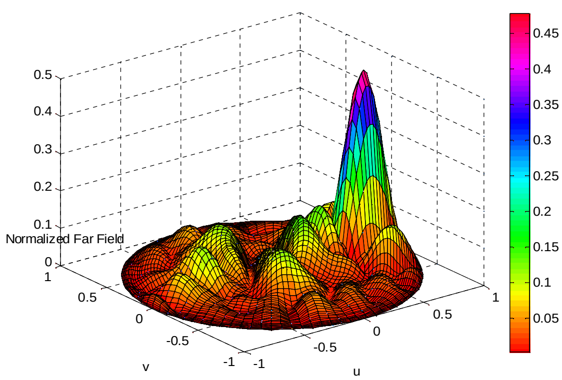

Table (11): *The excitation coefficients of each element, non-uniform excitation, theta 50 deg., DR= 10*

4.4791	14.928	5.7118	2.9167	10.107	10.213	5.4115	20.294
5.0944	19.004	12.280	24.454	3.1467	10.023	11.803	12.247
8.8712	12.900	9.6196	13.098	5.9269	17.652	25.410	20.751
12.275	9.8633	11.824	20.400	15.592	21.679	18.148	18.569
14.466	20.685	12.528	10.003	12.490	17.300	29.100	17.512
16.937	11.943	12.584	15.730	11.628	6.6292	13.434	9.9228
8.2905	23.833	8.4446	8.3443	15.843	15.266	24.243	17.607
9.6488	5.6477	9.5940	27.142	9.9308	25.602	3.5817	12.273

Figure (14): *The Normalized far field pattern at theta 55 deg., with non-uniform excitation.*